



Multiparticle Production in Reggeon Field Theory

J. BARTELS and E. RABINOVICI

Fermi National Accelerator Laboratory, Batavia, Illinois 60510

ABSTRACT

In the framework of reggeon field theory it is shown that multiparticle production processes with repeated Pomeron exchange satisfy unitarity constraints and avoid decoupling problems, for a small enough $\tilde{P}PP$ coupling. For a large $\tilde{P}PP$ coupling, the existence of a two-Pomeron bound state at $j > 1$ is discussed. We also find that the leading contribution to $\sigma_n(s)$ behaves like $\sigma_{el}(s)$.



The exposition of the strong coupling solution to Reggeon field theory (RFT)¹⁻³ has led to the investigation of many of its facets^{2,4,5} in an attempt to probe the extent to which RFT may serve as a consistent framework for large energy and small t behavior in strong interactions. One crucial test for RFT is the fulfillment of s -channel unitarity. By construction RFT's are t -channel unitary, but although they involve multipomeron cuts which have been used to enforce s -channel unitarity in absorptive models,⁶ it is not a priori clear that they satisfy all requirements of s -channel unitarity.

In the absence of a complete proof of s -channel unitarity, one is led to check whether RFT at least satisfies some of the constraints imposed by unitarity. One set of inelastic processes that are known to be problematical are the multiparticle production processes. In particular, the repeated exchange of a Pomeron pole with intercept one⁷ is known to violate the Froissart bound. It is, therefore, a severe test of RFT to see whether the Pomeron cut corrections in these processes restore s -channel unitarity.

In this letter we examine multiparticle production processes with repeated Pomeron exchange. Our calculations are based on reggeon field theory as derived from the reggeon calculus found recently.⁸ We compute $\sigma_n(s)$, $\sigma(s) = \sum_n \sigma_n(s)$ and find that s -channel unitarity is restored. The violation of the Froissart bound in the Finkelstein-Kajantie model is due to the existence of a j -plane singularity at $j > 1$, and we show that this

pole disappears in the presence of Pomeron cuts, provided the $\tilde{P}\tilde{P}\tilde{P}$ vertex (Pomeron-Particle-Pomeron vertex) is not too large. For large couplings the pole may persist. We then include a secondary reggeon into the production processes and demonstrate that decoupling problems are avoided. Details of all these calculations will be published elsewhere.

Part of this has been the subject of a study of Migdal, Polyakov, and Ter-Martirosyan.² Our results demonstrate that, in fact, they have considered only nonleading contributions to $\sigma_n(s)$ and, hence, do not answer the question of s-channel unitarity. Furthermore, our reggeon calculus allows us to include a secondary reggeon and study decoupling problems.

We first study the energy behavior of $\sigma_n(s)$ for processes with only Pomeron exchanges between produced particles (or clusters) with finite fixed masses (Fig. 1). Using the Lagrangian which describes the Pomeron in the elastic scattering¹ and treating the $\tilde{P}\tilde{P}\tilde{P}$ vertex as an external source for the Pomeron field, one obtains a scaling law for the $2 \rightarrow n$ scattering amplitude in the rapidity-impact parameter representation:

$$T_{2 \rightarrow n}(Y, Y_i; \vec{b}_i) = Y^{\beta - (n-1)\left(\frac{D}{2}z + \gamma + \beta\right)} \Phi\left(\frac{Y_i}{Y}, \frac{\vec{b}_i \vec{b}_j}{Y^z}\right) \quad (1)$$

where D is the transverse dimension ($D=2$ for the physical world), $Y = \ln s$ the total rapidity, $Y_i = \ln s_{i i+1}$ the rapidity gaps between the produced particles, and \vec{b}_i the impact parameter differences for the produced particles. The quantities β , γ , z denote the anomalous dimensions of the $\tilde{P}\tilde{P}\tilde{P}$ vertex, the Pomeron propagator, and the Pomeron slope, respectively. In the ϵ -expansion ($\epsilon = 4-D$) they are:

$$\beta = \epsilon/6, \quad \gamma = -\epsilon/12, \quad z = 1 + \epsilon/24 \quad . \quad (2)$$

The cross sections $\sigma_n(Y)$ for the production of $n-2$ particles are obtained from (1) by taking the square of its absolute value and integrating over the phase space of the produced particles \vec{b}_i , $\xi_i = Y_i/Y$. As long as we restrict ourselves to values of the order Y for the rapidity gaps, say $Y_i \geq c \cdot Y$, the ξ_i -integrations stay away from $\xi_i = 0$, and all integrations can be performed. The cross section coming from this region of phase space is

$$\sigma_n(Y) = \text{const} \cdot Y^{2\beta - (n-1)} \left(\frac{D}{2} z + 2\gamma + \beta - 1 \right) \quad (3)$$

in agreement with the results of Ref. 2. However, if we allow for values of Y_i which grow less rapidly than Y , say $Y_i \geq c Y^p$ ($0 < p < 1$), then the ξ_i -integration goes down to $c \cdot Y^{p-1}$ which becomes small for large Y and is sensitive to whether the ξ_i -integration converges for small ξ_i or not. We illustrate this for the Finkelstein-Kajantie case (i.e., no Pomeron cuts) in D dimensions ($2 \leq D < 4$). (Note that for $D > 2$ a kinematical softening factor $t^{(D-2)/4}$ is provided for the $\tilde{P}\tilde{P}\tilde{P}$ vertex.) After integrating

over the momentum transfers t_i we are left with the integrals over the rapidity gaps:

$$\sigma_n(Y) = \text{const} \cdot \int \prod dY_i \delta\left(\sum Y_i - Y\right) \prod_{Y_i}^{-1/D/2} \quad (4)$$

For $Y_i \geq cY$ we clearly have

$$\sigma_n(Y) = \text{const} \cdot Y^{-1-(n-1)(\frac{D}{2}-1)} \quad , \quad (5)$$

whereas $Y_i \geq cY^p$ leads to

$$\sigma_n(Y) = \text{const} \cdot \left\{ \begin{array}{ll} Y^{-1-(\frac{D}{2}-1)-(n-2)p(\frac{D}{2}-1)} & 2 < D < 4 \\ Y^{-1-(\frac{D}{2}-1)} (\ln Y)^{n-2} & D = 2 \end{array} \right\} \quad (6)$$

which is larger than the contribution (5). From (6) we see that $\sigma_n(Y)$ obtains its most important contribution from that region of phase space where the Y_i grow as little as possible (p small), i.e., in the most favored configuration of particle production all rapidity gaps but one are as small as allowed by phase space (or low energy dynamics). In the limit $p \rightarrow 0$ (Y_i finite) the cross sections are

$$\sigma_n(Y) = c(n) \cdot Y^{-1-(\frac{D}{2}-1)} \quad , \quad (8)$$

and the asymptotic energy decrease is independent of n . In contrast to this, the result (7) does not depend on p , and the important region of phase space is that where all Y_i are large.

Returning to our case, a close look at the scaling function Φ in (1)

tells us that, in going from (1) to σ_n , we encounter a divergent ξ_1 -integration, and expect that (3) will not be the dominant contribution to σ_n . Therefore, instead of squaring and integrating the scattering amplitude (1), we proceed differently and start from a reggeon field theory that describes directly the cross sections $\sigma_n(Y)$ rather than the scattering amplitude. The Lagrangian of this field theory is

$$\mathcal{L} = \sum_{i=1,2} \left[\frac{i}{2} \psi_i^\dagger \overleftrightarrow{\partial}_t \psi_i - \alpha'_0 \nabla \psi_i^\dagger \cdot \nabla \psi_i - a_0 \alpha'_0 (\nabla \psi_i^\dagger \cdot \nabla \psi_i)^2 - \Delta_0 \psi_i^\dagger \psi_i - \frac{ig_0}{2} (\psi_1^\dagger \psi_1^2 + \text{h.c.}) \right] - U_0 \psi_1^\dagger \psi_2^\dagger \psi_1 \psi_2, \quad (9)$$

where we have included a $(k^2)^2$ -term into the Pomeron trajectory in order to make the theory renormalizable at $D=4$. This term will not effect the infrared behavior of the Pomeron self-coupling.¹⁰ Together with two source terms, this Lagrangian describes the diagrams of Fig. 2, i.e., our theory takes into account all enhanced Pomeron absorptive corrections. The coupling g_0 describes the self-interaction of the Pomeron, and U_0 is the square of the $\underline{P}\underline{P}\underline{P}$ vertex. The divergence problems we have encountered above now appear as divergent integrations of Feynman diagrams, and are removed by standard methods of field theory. The objects of our interest are the cross sections $\sigma_n(Y)$:

$$\sigma_n(Y) = \frac{1}{2\pi i} \int dE e^{-YE} \sigma_n(E) \quad (10)$$

where E is the reggeon energy passing the diagrams of Fig. 2, and $\sigma_n(E)$ represents the sum of all graphs proportional to U^{n-1} (U is the

renormalized version of U_0 in (9)). Based on this Lagrangian we first derive, using renormalization group techniques, a scaling law for

$$\sigma(E) = \sum_n \sigma_n(E) \quad (11)$$

in the infrared region. The quartic coupling is infrared free,¹¹ and the behavior of $\sigma(E)$ is determined to be:

$$\sigma(E) \sim E^{-\left[1-2\gamma-z\frac{D}{2}\right]} \cdot \text{const} \quad (12)$$

with the exponent $1-2\gamma-z\frac{D}{2} = \frac{1}{6}$ in the ϵ -expansion Eq. (2). The partial cross sections σ_n are obtained by expanding the solution of the renormalization group equation of $\sigma(E)$ in powers of U and then considering the infrared behavior of the coefficients. The leading term is

$$\sigma_n(E) \underset{E \rightarrow 0}{\sim} \text{const} \cdot U^{n-2} E^{-\left[1-2\gamma-\frac{D}{2}z\right]} \quad (13)$$

The important feature of this result is that all $\sigma_n(E)$ have the same infrared behavior (except for different constants) and lead to the cross sections:

$$\sigma_n(Y) \sim \sigma_{el} \sim (\ln s)^{-\frac{5}{6}} \quad (14)$$

The contribution (3) to $\sigma_n(Y)$ is given by one of the nonleading terms in the infrared expansion of $\sigma_n(E)$. The physical picture for (14), as opposed to (3), is the same as the one described after (6): the dominant part of $\sigma_n(Y)$ is given by a configuration of particle production where one rapidity gap is of the order Y , while the others are as small as allowed by phase space, or some low energy dynamics. In this calculation we have not included nonenhanced graphs which for finite (however arbitrarily large) rapidities

Y_i are no longer negligible. However, the fact that for large s all but one rapidity gap are pushed to their lower limit is dictated by the enhanced graphs, and nonenhanced graphs would not effect this behavior.

From (12) we know already that, for $E \sim 0$, $\sigma(E)$ behaves like $\sigma_n(E)$ and hence the contribution to $\sigma_n(Y)$, due to the region $E \sim 0$, is not larger than σ_{el} . So there is no violation of unitarity, since $\sigma_{el} < \sigma_{tot}$. However, this does not yet guarantee that our theory avoids the Finkelstein-Kajantie problem which has its origin in the existence of a j -plane singularity to the right of $j = 1$. In order to illustrate this in more detail, we drop in our Lagrangian (9), the Pomeron self-interaction g_0 , which leads us back to the Finkelstein-Kajantie situation without Pomeron cuts. For this case we can explicitly compute $\sigma(E)$:

$$\sigma(E) = \frac{U}{1 + U \cdot I(E)} \quad (15)$$

with

$$I(E) = \text{pos. const} \times \left[\frac{\ln \frac{1 - \sqrt{1 + \frac{2aE}{\alpha'}}}{1 + \sqrt{1 + \frac{2aE}{\alpha'}}}}{\sqrt{1 + \frac{2aE}{\alpha'}}} - \frac{\ln \frac{1 - \sqrt{1 - \frac{2aE_N}{\alpha'}}}{1 + \sqrt{1 - \frac{2aE_N}{\alpha'}}}}{\sqrt{1 - \frac{2aE_N}{\alpha'}}} \right] \quad (16)$$

(E_N is some constant renormalization energy) From this we learn that $\sigma(E)$ has a pole at some negative $E = 1-j$, no matter how large or small U , and the Finkelstein-Kajantie disease is reflected as a pole in the j -plane to the right of $j = 1$. If our theory is to avoid the inconsistency,

we have to show that this pole disappears once the Pomeron self-interaction is turned on. We do this by taking a closer look at the β -function which describes the behavior of $U(\ln E)$ in the renormalization group equation for $\sigma(E)$. In the absence of the triple Pomeron coupling it is possible to calculate $\beta(U)$ explicitly, and we show its behavior as a function of U in Fig. 3a for both $D = 2$ and $2 > D \leq 4$. Using the argument of Gross and Neveu,¹² it is possible to read off the existence of a two-Pomeron bound state from the behavior of $\beta(U)$. First take $D > 2$, where we know that a kinematical softening of the $\tilde{P}\tilde{P}\tilde{P}$ vertex is provided. β starts with a positive slope at $U=0$, but eventually turns over, has another zero at U_c and goes like $U^2 \times \text{negative const.}$ for large U . If now the physical value U sits to the right of U_c , there exists a bound state, whereas for $0 < U < U_c$ this bound state disappears.¹³ Next we let D approach 2: as it can be seen in Fig. 3, the interval $[0, U_c]$ becomes smaller and smaller, and at $D=2$ it is shrunk to zero. So at $D=2$, there are no values for U , for which the pole is absent.

Now we turn on the Pomeron self-interaction g (Fig. 3b). Then $\beta(U)$ becomes a function of g^2 as well. For D equal or close to 4, β only slightly differs from the situation without the triple pomeron coupling, because g^2 is effectively small of the order $\epsilon = 4-D$. As in the previous case, we therefore have a region for U , in which we are not plagued with any bound state pole, but for U large enough such a pole exists. If

D approaches 2, we lose any control over the β -function for large U , but we retain the information (at least in order g^2) that the slope of β at $U=0$ remains positive and different from zero (this is what makes the point $U=0$ infrared stable). This guarantees that the region of allowed U values for which no pole exists remains different from zero at $D=2$. Whether we still have a pole for large enough U depends on the behavior of β for large U .

It is interesting to note that the slope r of $\beta(U)$ at $U=0$ has a simple interpretation. It is given by

$$r = 2\gamma + 2\beta - \frac{D}{2}z - 1 \quad (17)$$

with γ, β, z defined in (2). If we think of a production process with the exchange of only one (renormalized) Pomeron between two neighborhood (renorm.) $\tilde{P}\tilde{P}\tilde{P}$ vertices, then a simple counting of anomalous dimensions leads to (cf. (4))

$$\sigma_n = \text{const} \cdot \int \prod dY_i \delta \left(\sum Y_i - Y \right) \frac{1}{Y_i^{1+r}} \quad (18)$$

Thus a positive r , resulting from this simple power counting already indicates the behavior of β near $U=0$.

We conclude from this that, in the presence of a triple Pomeron coupling, the two-Pomeron bound state which causes the Finkelstein-Kajantie disease has moved away as long as the value of the $\tilde{P}\tilde{P}\tilde{P}$ vertex does not exceed a certain critical value. If the vertex is large enough, then we know, at least for $D \sim 4$, that the bound

state does exist. Thus Pomeron cuts do cure the Finkelstein-Kajantie disease of the simple Pomeron pole picture. But at the same time, s-channel unitarity seems to restrict the range of permitted values for the $\tilde{P}\tilde{P}\tilde{P}$ vertex, as long as we do not take into consideration other possible mechanisms to remove the singularity at $j > 1$.

In order to complete our plan, we have to show that the way in which s-channel unitarity is restored does not lead to any decoupling problems. The basic mechanism which in our model reconciles the repeated Pomeron exchange with s-channel unitarity is the screening of the $\tilde{P}\tilde{P}\tilde{P}$ vertex. The radiative corrections produce an anomalous dimension:

$$\Gamma_{\tilde{P}\tilde{P}\tilde{P}}\left(\xi \frac{E_1}{E_N}, \xi \frac{E_2}{E_N}, \vec{k}_1, \vec{k}_2\right) \underset{\xi \rightarrow 0}{\sim} \xi^\beta \psi\left(\frac{E_1}{E_N}, \frac{E_2}{E_N}, \alpha' \frac{\vec{k}_1 \cdot \vec{k}_2}{\xi^z E_N}\right), \quad (19)$$

where E_1 , E_2 and \vec{k}_1 , \vec{k}_2 are energy and momentum of the adjacent Pomerons, and z and β are given in (2). Next we repeat the argument⁹ which in the case of a $\tilde{P}\tilde{P}\tilde{P}$ vertex of the form $\Gamma_{\tilde{P}\tilde{P}\tilde{P}}(t_1, t_2) \sim at_1 + bt_2$ leads to the decoupling of the Pomeron from the total cross section.

We take the produced objects in Fig. 1 to be pairs of particles with sufficiently large subenergies, such that between them a secondary Regge pole with nonzero momentum t_R is exposed. This leads to the diagrams of Fig. 4. Among all possible diagrams we consider only those which contribute to the Regge pole exchange, and drop all those which lead only to Regge-Pomeron cuts in the Reggeon channel. This eliminates diagrams with Pomerons going all the way parallel to a reggeon from the one side

of a particle pair to the other. If the remaining diagrams are to satisfy s-channel unitarity in the same way as the processes we considered above, each renormalized $\tilde{P}PR$ vertex must be screened by itself, and this screening must be strong enough. Otherwise one would either have to show that the addition of all cut contributions in the reggeon channel would restore unitarity, which because of the different t -behavior of Regge pole and Regge-Pomeron cuts is not likely to be true for all values of t_R . Alternatively, one could assume a vanishing bare $\tilde{P}PR$ coupling. This, however, leads back to the decoupling difficulties. For although we do not know how to continue our reggeon calculus from negative t_R to positive values, we do know⁸ that at the particle pole ($t_R = m^2$ and physical angular momentum) all Pomeron cut-contributions must decouple from the physical partial wave. Hence only the bare $\tilde{P}PR$ vertex survives, and its vanishing at negative t_R would lead to the old difficulties.

A closer look at the $\tilde{P}PR$ vertex with the reggeon on its energy momentum shell shows that radiative Pomeron corrections as shown in Fig. 5 produce branch points in the Pomeron energy plane which accumulate at zero when the Pomeron momentum goes to zero. It is important to note that such an accumulation, which is known to take place when both Pomeron and Reggeon are infrared, also holds for $t_R \neq 0$, as long as the reggeon sits on its energy shell. For our argument, we take $t_R \neq 0$.

The $\tilde{P}PR$ vertex is described by a reggeon trajectory

$$\alpha_R[(Q+k)^2] = \alpha_R[Q^2] + 2\beta' \vec{Q} \cdot \vec{k} \quad (20)$$

and a Lagrangian

$$\begin{aligned} \mathcal{L} = & \frac{i}{2} \psi^\dagger \overleftrightarrow{\partial}_t \psi - \alpha_0' \nabla \psi \cdot \nabla \psi - \Delta \psi^\dagger \psi - \frac{ig_0}{2} (\psi^\dagger \psi^2 + \text{h.c.}) \\ & + \frac{i}{2} \phi^\dagger \overleftrightarrow{\partial}_t \phi - \left[2\beta' \phi^\dagger \vec{Q} \cdot \nabla \phi + \text{h.c.} \right] \\ & - iV_0 \psi^\dagger \phi^\dagger \phi \quad . \end{aligned} \quad (21)$$

Here ψ , ϕ are Pomeron and reggeon fields, respectively, and the reggeon, being close to its energy shell, carries energy and momentum $\Omega + E_2$, $\vec{Q} + \vec{k}_2$ with $\Omega = 1 - \alpha_R(Q^2)$, $t_R = -Q^2$. The Lagrangian (19) is constructed to reproduce the correct infrared behavior of the Pomeron variables.

Application of the standard renormalization group techniques leads to the result that the $\tilde{P}PR$ -vertex has the behavior

$$\Gamma_{\tilde{P}PR} \left(\xi \frac{E_1}{E_N}, E_2=0, \vec{k}_1, \vec{k}_2=0 \right) \sim \xi^{-\frac{1}{2}\gamma} \cdot f \left(\frac{E_1}{E_N}, \alpha' \frac{\vec{k}_1^2}{E_N \xi^2} \right) \quad (22)$$

with γ being the anomalous dimension of the Pomeron propagator. (This result holds in all orders of perturbation theory.) Thus the renormalized \tilde{P} -two particle- \tilde{P} vertex with a Regge pole exchange between the two particles has a behavior similar to (17) with the anomalous dimension $-\gamma$. Proceeding now with the production of n such pairs in the same way as we did with processes of Fig. 1, we find that this screening is sufficient to satisfy s-channel unitarity.

In conclusion, we have demonstrated how RFT in multiparticle production processes obeys s-channel unitarity constraints and avoids decoupling problems. We also found that in the leading contribution to $\sigma_n(s)$ only one rapidity gap is large. Accordingly, $\sigma_n(s)$ has asymptotically the same energy dependence as $\sigma_{el}(s)$.

ACKNOWLEDGMENTS

For helpful discussions we would like to thank H. D. I. Abarbanel, J. Carazzone, J. Cardy, M. Einhorn and A. Schwimmer.

REFERENCES AND FOOTNOTES

- ¹H. D. I. Abarbanel and J. B. Bronzan, Phys. Rev. D9, 2397 (1974).
- ²A. A. Migdal, A. M. Polyakov, and K. A. Ter-Martirosyan, Phys. Lett. 48B, 239 (1970) and Zh. Eksp. Teor. Fiz. 67, 87 (1974).
- ³For an extensive review on reggeon field theory see H. D. I. Abarbanel, J. B. Bronzan, R. L. Sugar, and A. R. White, Physics Report, to be published.
- ⁴J. L. Cardy and R. L. Sugar, Preprint 1975.
- ⁵H. D. I. Abarbanel, J. Bartels, J. B. Bronzan, and D. Sidhu, to be published.
- ⁶For the most recent work on this line see M. Ciafaloni and G. Marchesini, Nucl. Phys. B88, 109 (1975).

- ⁷I. A. Verdiev, O. V. Kanchelli, S. G. Martinyan, A. M. Popova, and K. A. Ter-Martirosyan, Zh. Eksp. Teor. Fiz. 46, 1700 (1964) [Sov. Phys. JETP 19, 1148 (1964)] .
J. Finkelstein and K. Kajantie, Nuov. Cim. 56A, 659 (1968) and Phys. Lett. 26B, 305 (1968).
- ⁸J. Bartels, FERMILAB-Pub-74/94 and 95-THY, to appear in Phys. Rev. D11.
- ⁹For a review on decoupling theorems see R. C. Brower, C. E. DeTar, and J. H. Weis, Physics Reports 14, 257 (1974).
- ¹⁰R. C. Brower and J. Ellis, Phys. Letters 51B, 242 (1974).
- ¹¹The infrared freedom of the quartic Pomeron coupling has been shown by H. D. I. Abarbanel and J. B. Bronzan, Phys. Rev. D9, 3304 (1974), W. A. Bardeen, J. W. Dash, S. S. Pinsky, and V. Rabi, preprint C00-1545-155. Note, however, that our Lagrangian (9) does not include all diagrams that occur in these papers.
- ¹²D. J. Gross and A. Neveu, Phys. Rev. D10, 3235 (1974). See also D. J. Gross and F. Wilczek, Phys. Rev. D8, 3633 (1973).
- ¹³For $0 < U < U_c$ the bound state has moved into the complex E-plane and sits on an unphysical sheet. Details will be given in a more extensive version of our results.

FIGURE CAPTIONS

- Fig. 1 Multiparticle production with repeated Pomeron exchange and Pomeron cut corrections.
- Fig. 2 Diagrams for the cross section $\sigma_n(s)$.
- Fig. 3 The function $\beta(U)$ for $D=2$ and $2 < D \leq 4$.
- (a) no Pomeron self-interaction.
- (b) with Pomeron self-interaction.
- Fig. 4 Production of n -particle pairs with Regge pole exchange in the two-particle pair. The wavy line denotes Pomerons, the zigzag line secondary reggeons.
- Fig. 5 Radiative corrections to the $\tilde{P}PR$ vertex

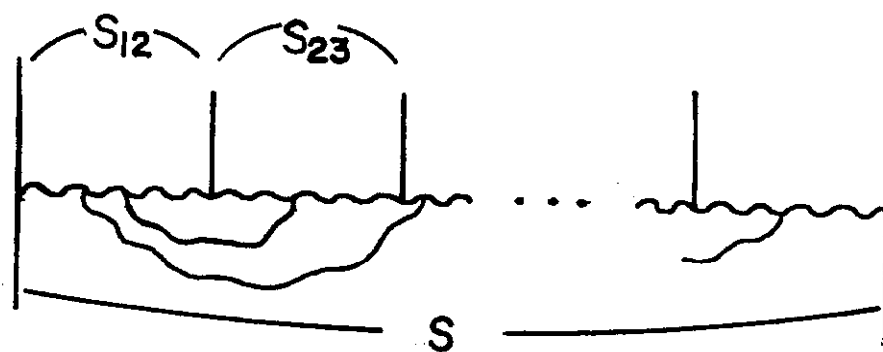


Fig. 1

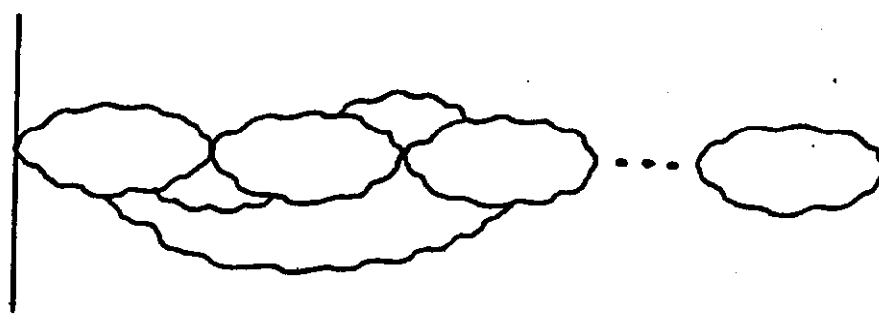
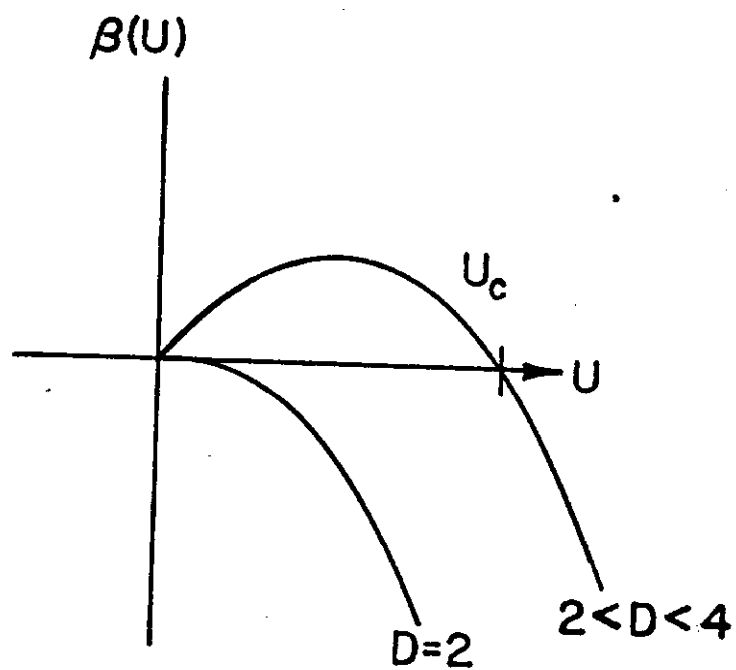
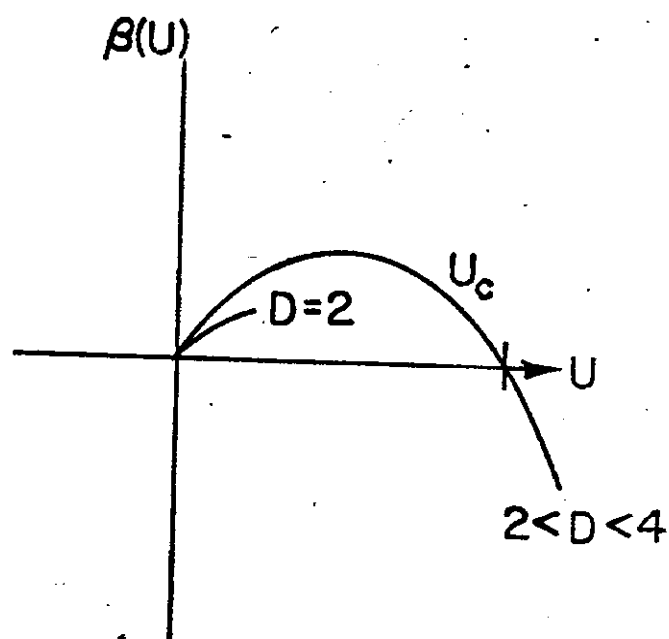


Fig. 2



(a.)



(b.)

Fig. 3

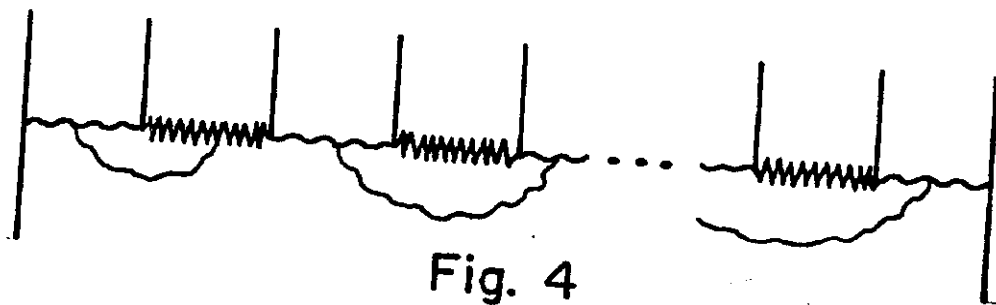


Fig. 4

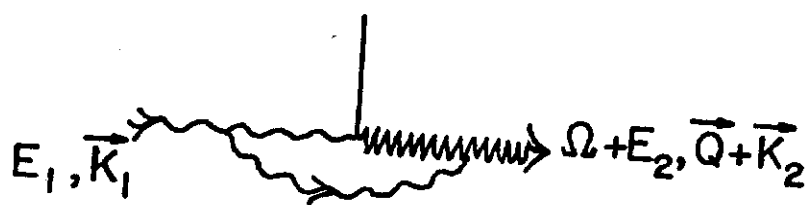


Fig. 5